SAND2014-20192C

Spectroscopic Temperature Inferences from Downward Burning Solid Rocket Propellants

D.M. Surmick*, A.D. Haug, C.G. Parigger*, A.B. Donaldson, and W. Gill

*University of Tennessee Space Institute, Tullahoma, TN

December 11th , 2014

Outline

- Introduction
- Experimental Summary
- Calculation of Diatomic AlO Spectra
- Thermal Continuum Analysis
  - Wavelength Dependent Emission Models
- Results
- Summary/Future Considerations

Introduction

- The goal is to use optical emission spectroscopy to probe solid propellant plumes to determine the temperature field
  - Relatively Noninvasive and Relatively Easy
- Diatomic AlO emissions are used to infer the temperature of aluminum particles
  - AlO observed from the flame surrounding individual Al particles
- Thermal continuum emissions are used to characterize the flame temperature

Experimental Summary

- Probe was inserted into propellant plume to measure emission spectra at various positions
- Fiber coupled spectrometer collected narrowband (460-530 nm) and broadband (500-950 nm) spectral data
- Investigated several gap heights and substrate materials

Test Set Up

- Varied position of probe within each test (~1-2 in.)
- Varied position of probe from test to test (~2-12in)

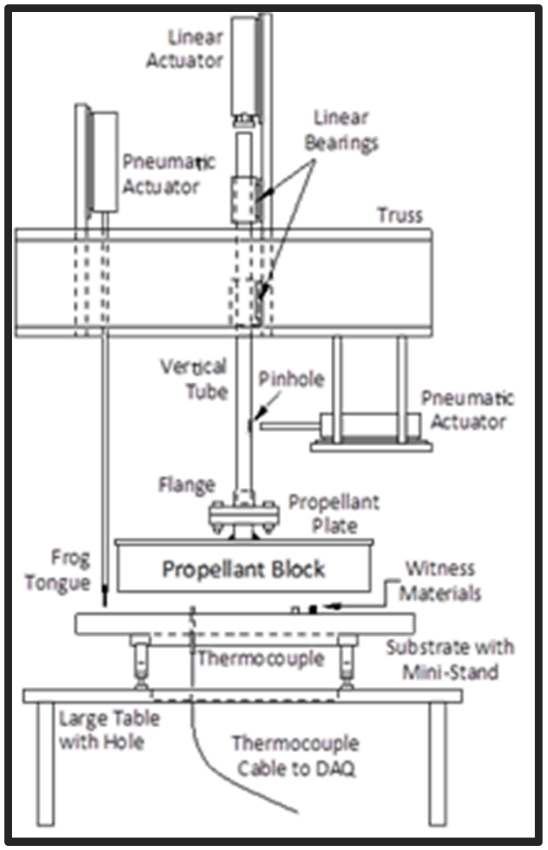

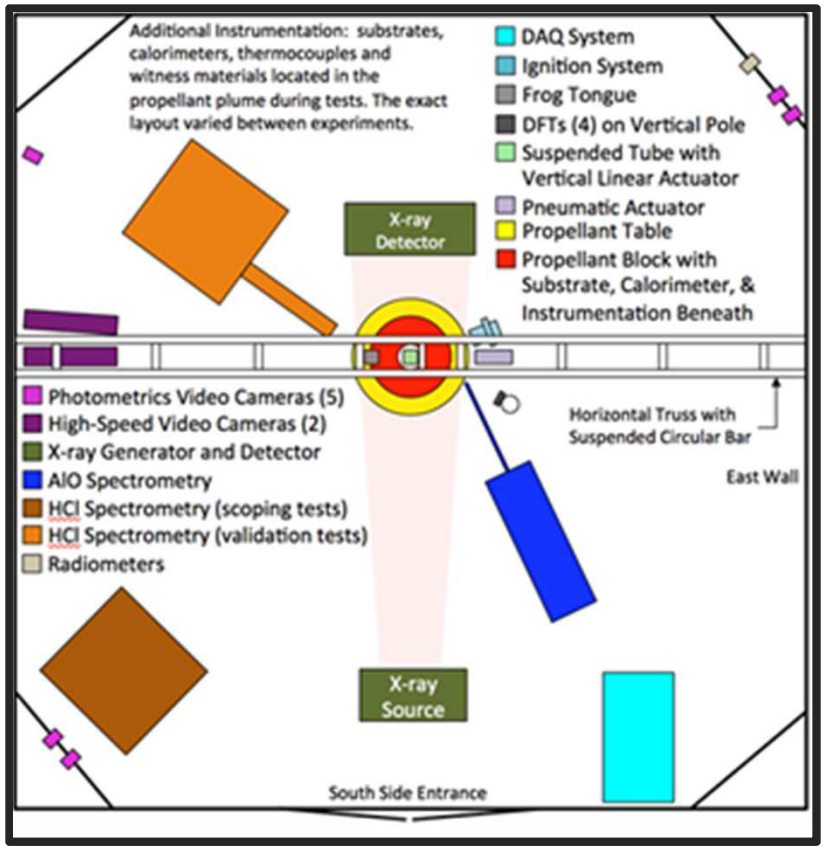

Data Reduction

Data are analyzed in five steps

1. Spectral data are visualized
2. Calibrated for detector sensitivity and background
3. Analyze AlO spectra for the B $^2\Sigma^+ \rightarrow$X $^2\Sigma^+$ transition
4. Analyze background thermal emissions for wavelength dependent emissivity
5. Comparisons are made between fitting models

Spectral Calibration

- Prior to analysis all spectra are properly calibrated for detector response and sensitivity
- Xe, Hg, Ar, Ne pen-ray lamps for detector response
- Halogen light source for detector sensitivity

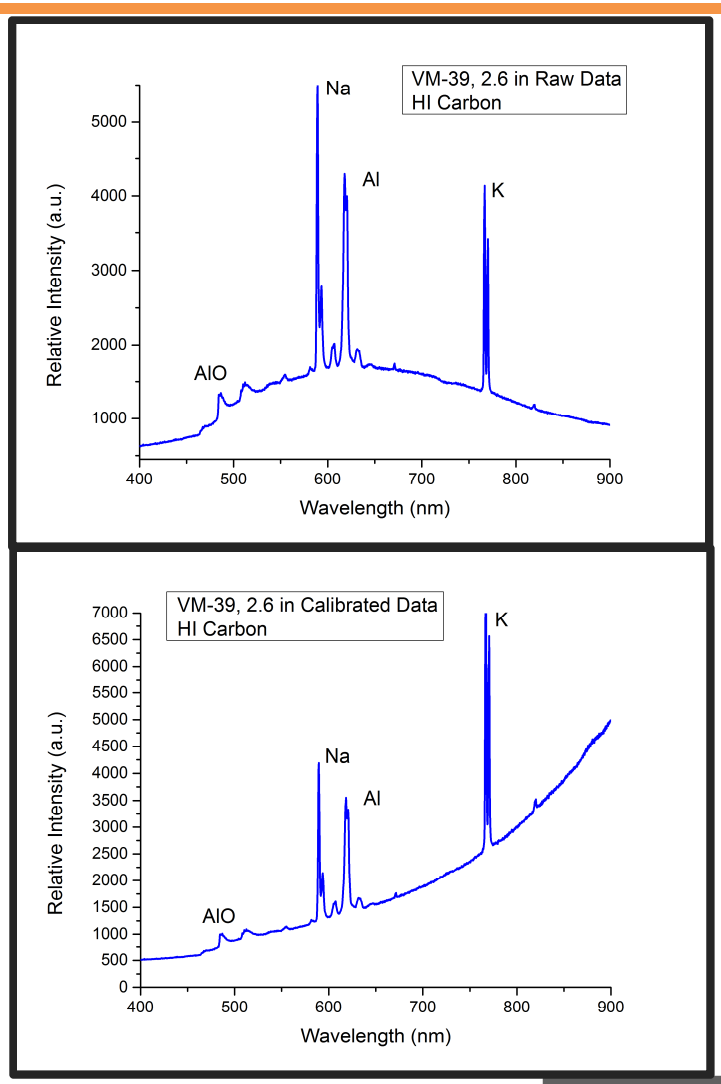

Calculation of Diatomic Spectra

Recipe for calculating diatomic spectra

1. Calculate positions of all possible transitions
2. Invoke electronic selection rules;
3. Calculate Hönl-London factors $S(J',J)$;
4. Calculate upper and lower energy level potentials;
5. Determine Franck-Condon factors $q(v',v)$;
6. Evaluate r-centroids, combine with FCF to form S_{elec}
7. Product of HLF and of electronic transition strength, S_{elec} , yield total line strength.

Calculation of Diatomic Spectra

AlO emission spectra are calculated using diatomic line strengths, S_{ul}, for transitions from upper state, u, to lower state , l, [14]

$$S_{ul} = \sum_u \sum_l \left| \left\langle u \left| \hat{T}_k^{(q)} \right| l \right\rangle \right|^2, \quad \hat{T}_k^{(q)} \ldots \text{ Electric Dipole Operator}$$

Analytically calculate line strength in factorized form:

$$S_{ul}(n'v'J'M', nvJM) = S_{elec}(n'v', nv)S(J', J)$$

Model the intensity, (I_{ul}) incident on a detector pixel as

$$I_{ul} = \frac{16\pi^3 c(a_0 e)^2 v^4}{3\varepsilon_0 Q} N_0 C_{abs} C_v \tilde{\nu}_{ul}^4 S_{ul} \exp\left(\frac{-hF_u}{k_B T}\right)$$

Leads to a simple yet rigorous selection rule

- **Allowed Transitions have Non-Vanishing Line Strengths**

Calculation of Diatomic Spectra

High resolution AlO B-X Δv = 0

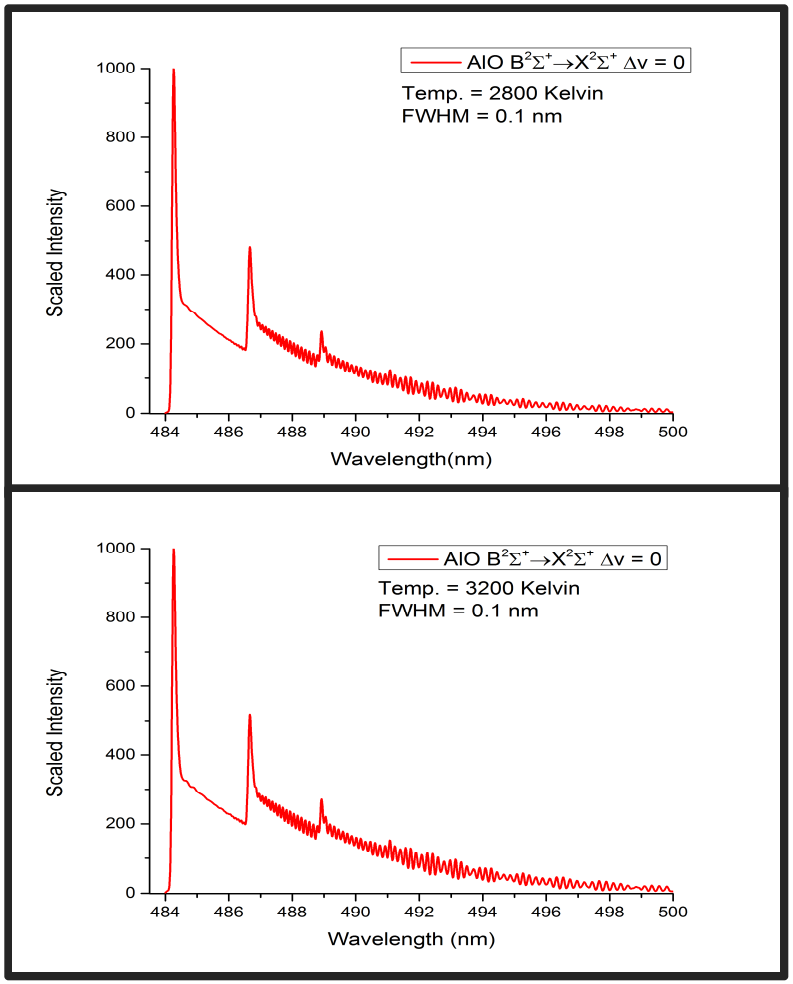

Lower Resolution AlO B-X

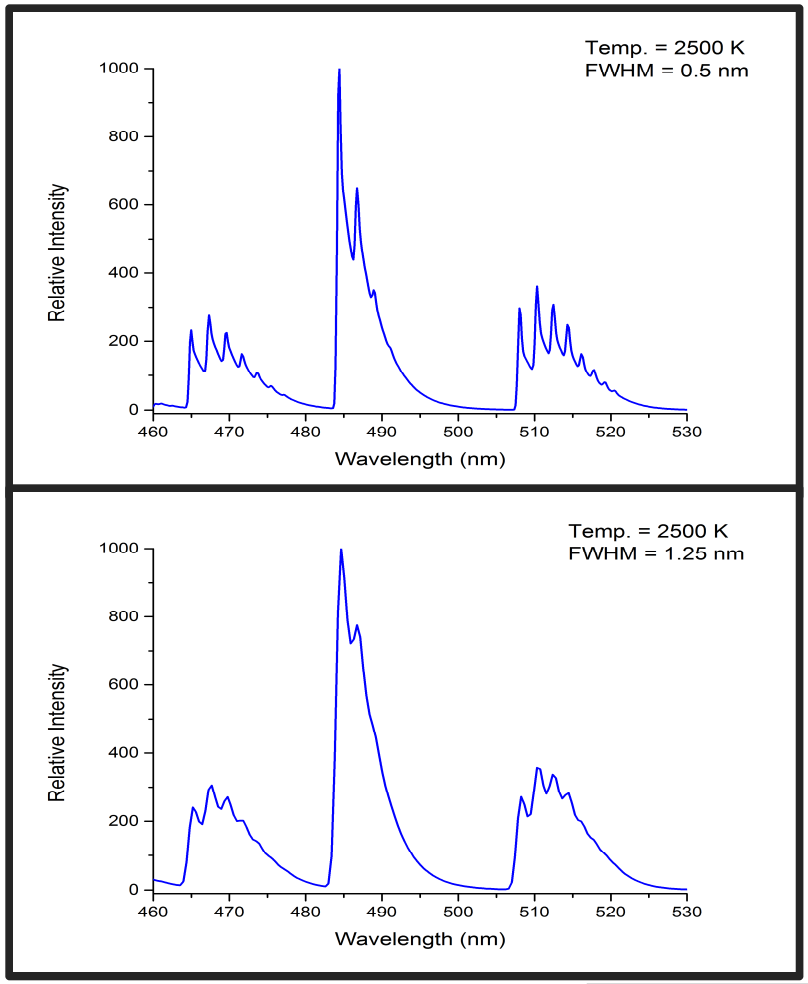

Fitting Algorithm

- Use the Nelder-Mead algorithm to fit diatomic spectra to theoretical calculations of spectra
- Utilizes a downhill, simplex fitting method to minimize input parameters
- Nelder-Mead algorithm chosen for its ability to fit multiple parameters simultaneously
  - Temperature, Baseline Offset, Spectral Resolution (FWHM)

AlO Emissions

- Error bars for AlO emissions are inferred by varying the resolution parameter

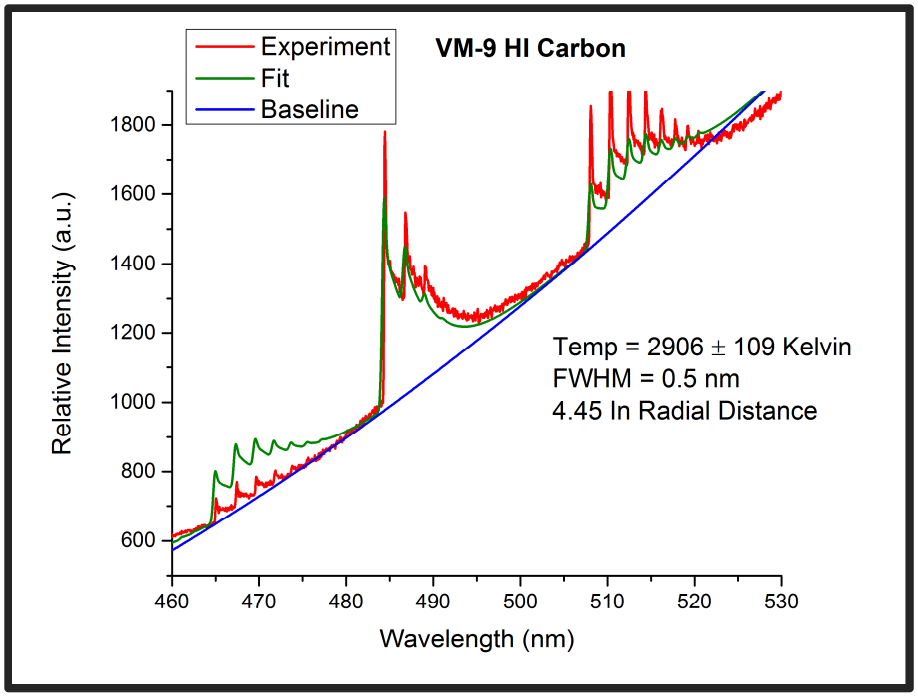

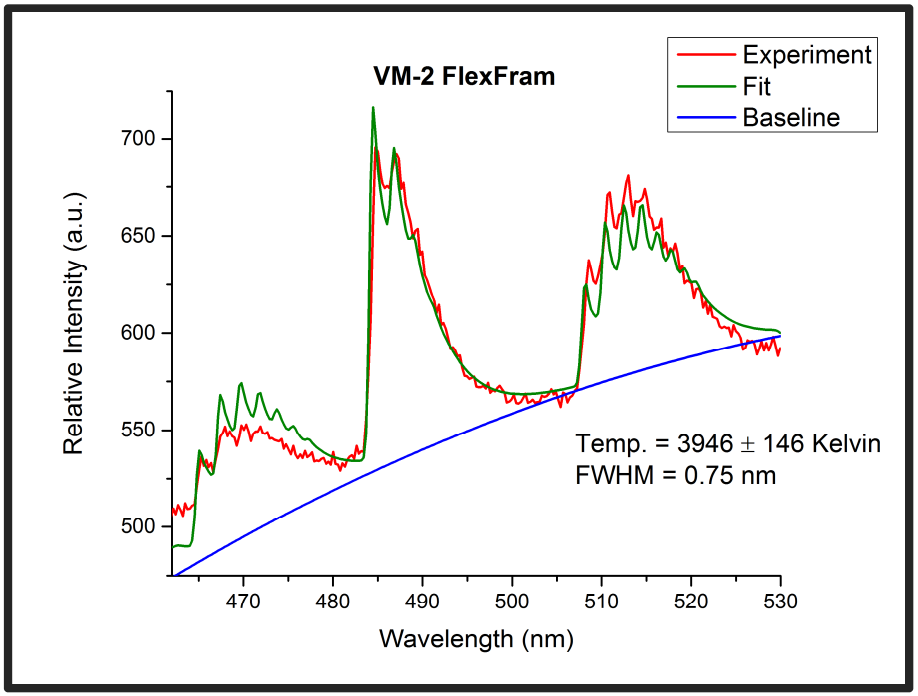

Wavelength Dependent Emissions

- Small particles, with a size distribution on the order of the wavelength of emission, indicate wavelength dependent emissivity [6].
- Use poly-logarithms, $Li_s(z)$, and Lambert functions, $W(z)$, to compute Wien's Displacement law [7]:

$$\lambda_{\max} \times T = \frac{hc}{k_B} \times \frac{1}{5 + W_0(-5e^{-5})} = 2.898 \times 10^6 \, nmK$$

Wavelength Dependent Emissions

Derivation of Wavelength Dependent Emission Model [7]

$$Li_s(z) = \sum_{k=1}^{\infty} \frac{z^k}{k^s}, |z| < 1$$

$$\frac{d}{dz}\left(Li_s(z)\right) = \frac{Li_{s-1}(z)}{z}$$

Consider

$$Li_1 = \sum_{k=1}^{\infty} \frac{x^k}{k} = -\ln(1-x)$$

Now apply to Planck's law

$$I(\lambda,T) = \frac{2\pi hc^2}{\lambda^5}\frac{1}{\exp(\beta)-1}, \beta = \frac{hc}{\lambda k_B T}$$

$$= \frac{2\pi hc^2}{\lambda^5} Li_0(\exp(\beta))$$

Maximize wrt λ to derive Wien's Law

$$5Li_0(e^{-\beta}) - \beta Li_{-1}(e^{-\beta}) = 0$$

$$(\beta - 5)e^{\beta-5} = -5e^{-5}$$

Solve using the Lambert Function

$$W(z)e^{W(z)} = z$$

$$\beta = 5 + W_0(-5e^{-5})$$

$$\lambda_{\max} \times T = \frac{hc}{k_B} \times \frac{1}{5 + W_0(-5e^{-5})}$$

Wavelength Dependent Emissions

- Applying the same method, we find:

$$\lambda_{\max} \times \overline{T} = 2.415 \times 10^6 \, nmK$$

and

$$\lambda_{\max} \times \overline{\overline{T}} = 2.070 \times 10^6 \, nmK$$

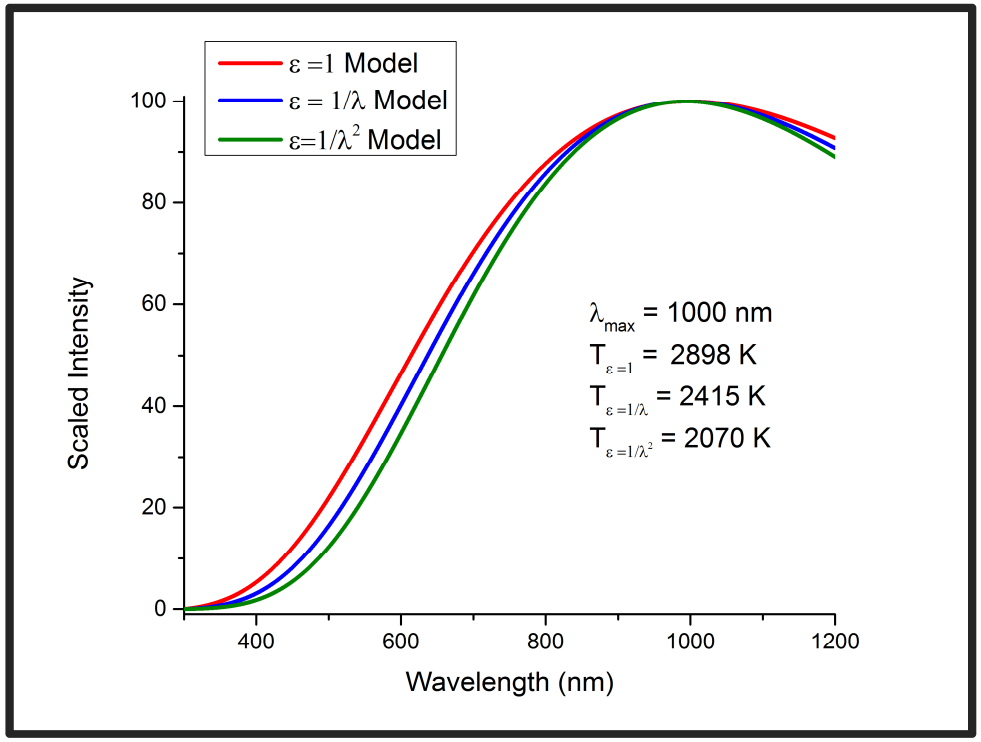

Planck Fitting

Wavelength dependency may be used with Planck's Law:

$$I(\lambda,T)=\frac{\varepsilon(\lambda,T)}{\lambda^5}\frac{2\pi hc^2}{\exp\left(\frac{hc}{\lambda k_B T}\right)-1}$$

Linearize, semi-log plot for fitting

$$\ln\left(\frac{I(\lambda,T)\times\lambda^5}{\varepsilon(\lambda,T)}\right)=-\ln\left(\exp\left(\frac{hc}{\lambda k_B T}\right)-1\right)$$

$$\ln\left(\frac{I(\lambda,T)\times\lambda^5}{\varepsilon(\lambda,T)}\right)\cong-\frac{hc}{k_B T}\frac{1}{\lambda}$$

Planck Fitting

- Only consider ε = 1, $1/\lambda$, $1/\lambda^2$ emissivity dependence (for now)
- Remove atomic and molecular emissions for straight line fitting
  - Al, AlO, Fe, Na, and K

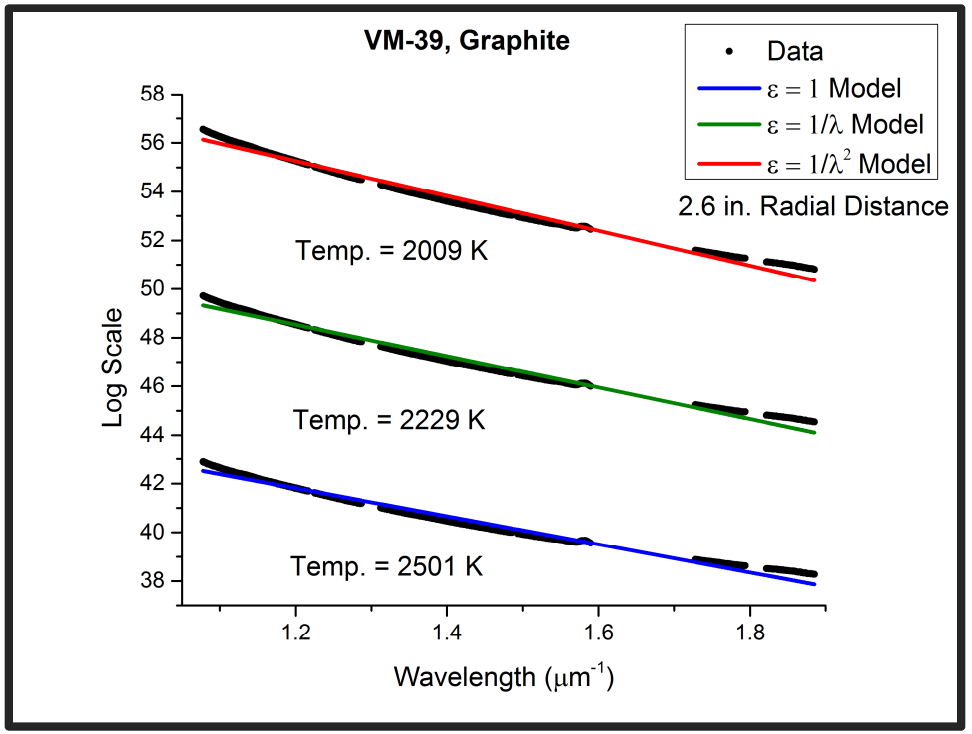

Results

Graphite, Wet Concrete, FlexFram, HI Carbon, Sandbed, Dry Concrete, Substrates

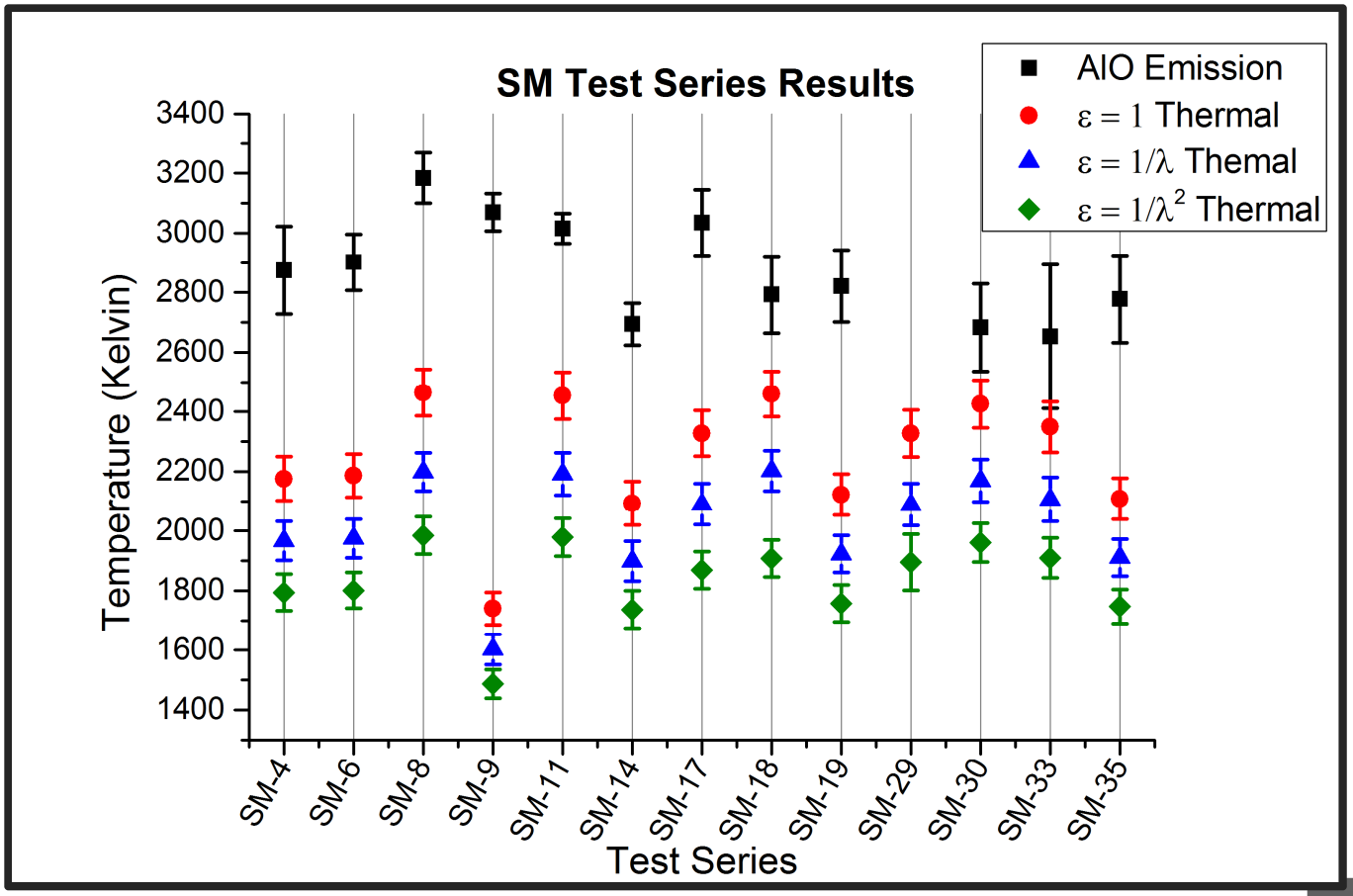

Results

Graphite, Wet Concrete, FlexFram, and HI Carbon Substrates

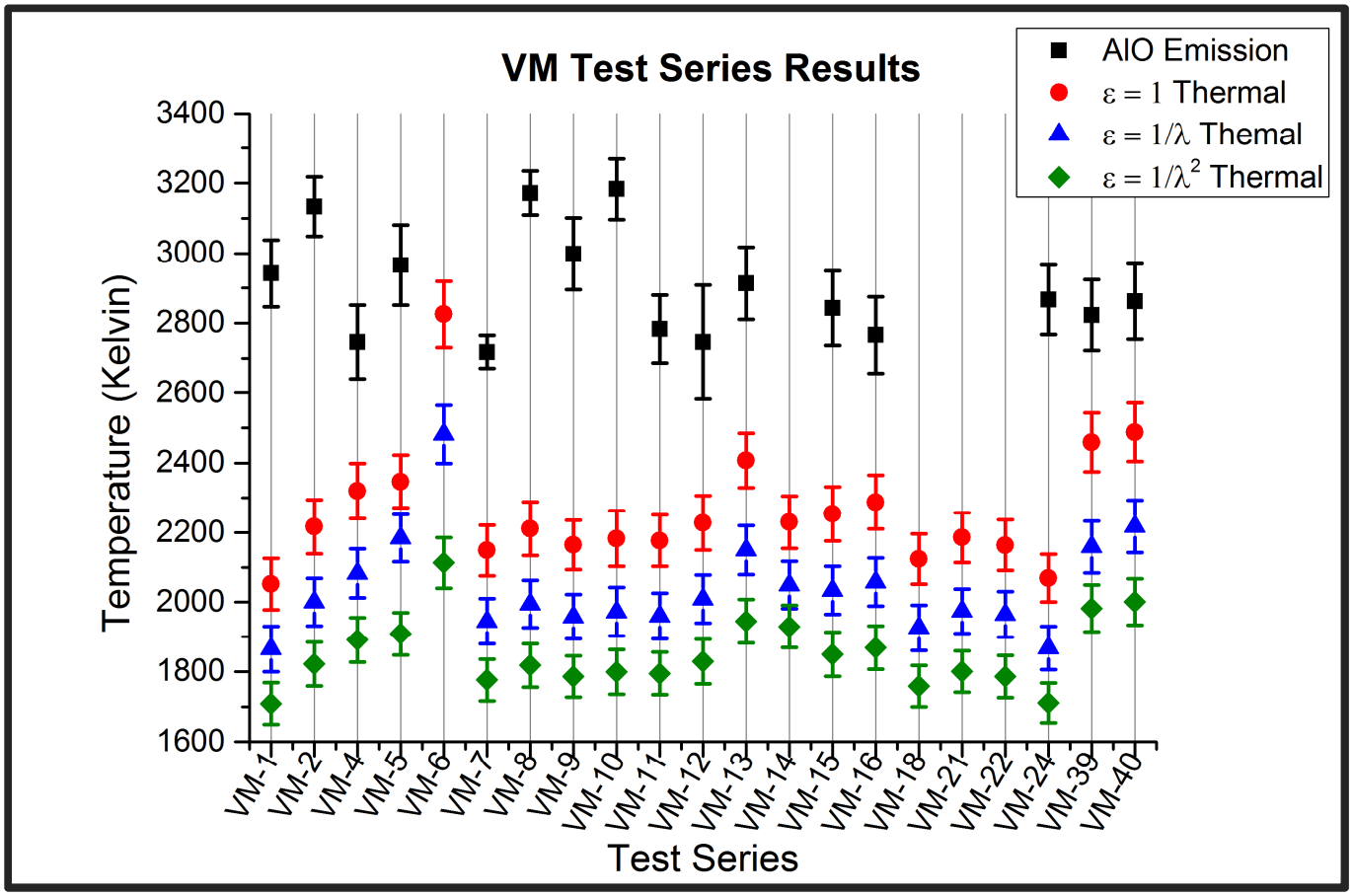

Results-Positional Dependence

- Slight positional dependence observed
- AlO emissions show larger variation over a data set than thermal emissions

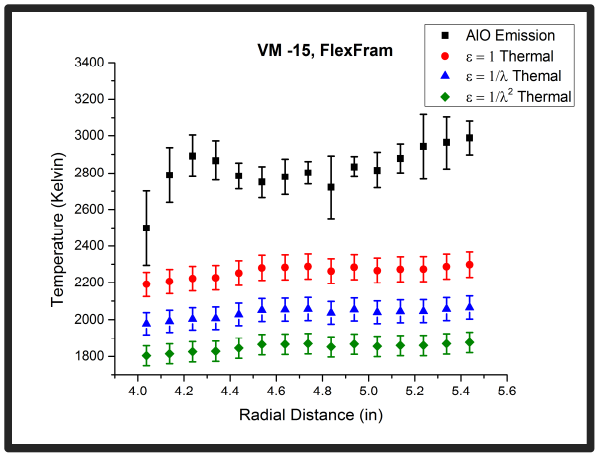

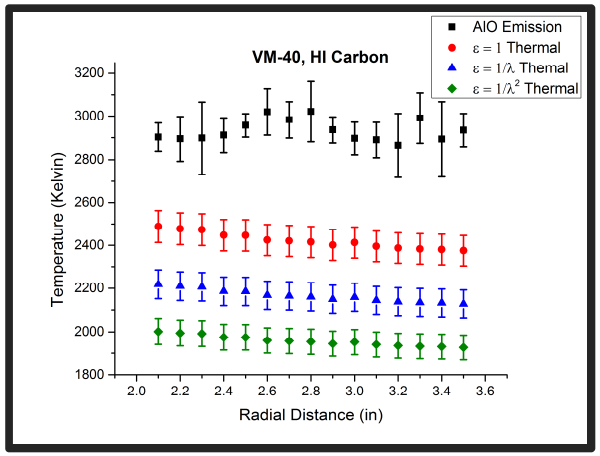

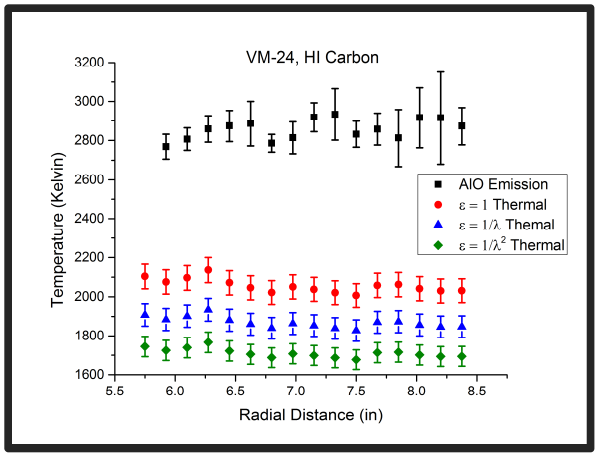

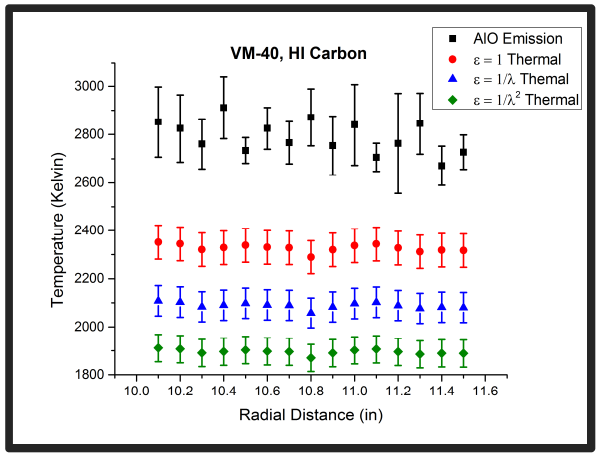

Results-Substrate Dependence

- Substrates are consistent within a temperature range
- 2800-3200 Kelvin for AlO emissions
- 2000-2400 Kelvin for thermal emissions

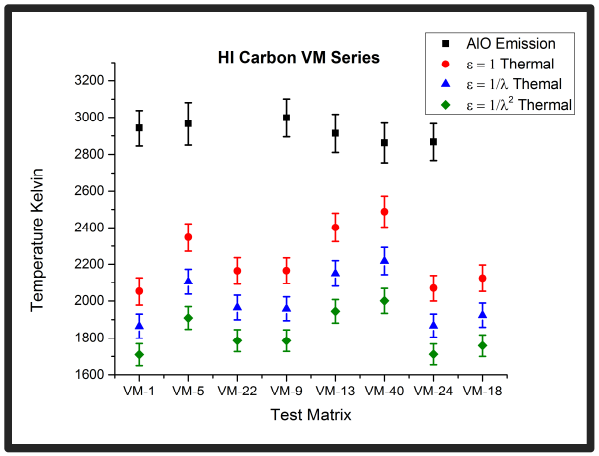

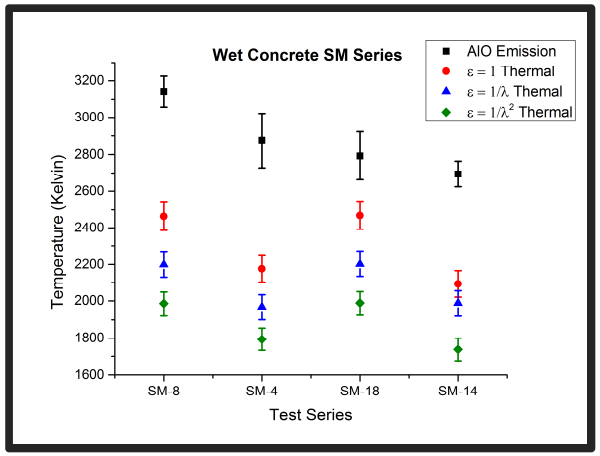

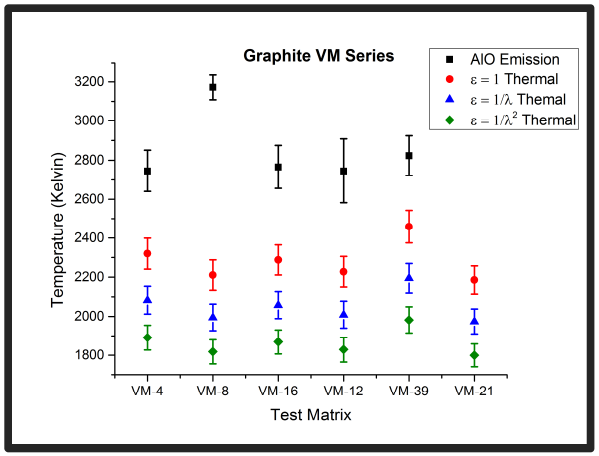

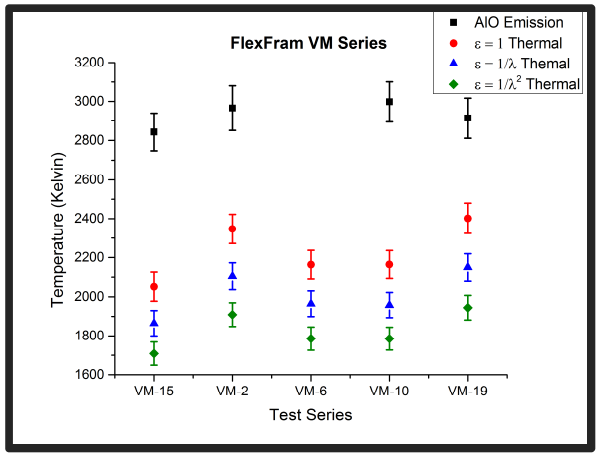

Summary

- Temperatures are fairly consistent with each other;
- Very few data sets showed positional dependence;
- Gap size and propellant size does not have an apparent effect on the temperature;
- Substrates appear to be consistent with each other
- AlO emission temperatures 2800-3200 Kelvin;
- Thermal emissions 2000-2400 Kelvin;
- Wavelength dependence of emissivity is of continued interest.

Future Considerations

- Continued laboratory scale testing
- Inclusion of HCl emissions with our diatomic line strength method
- Development of a species density diagnostic (LIBS)

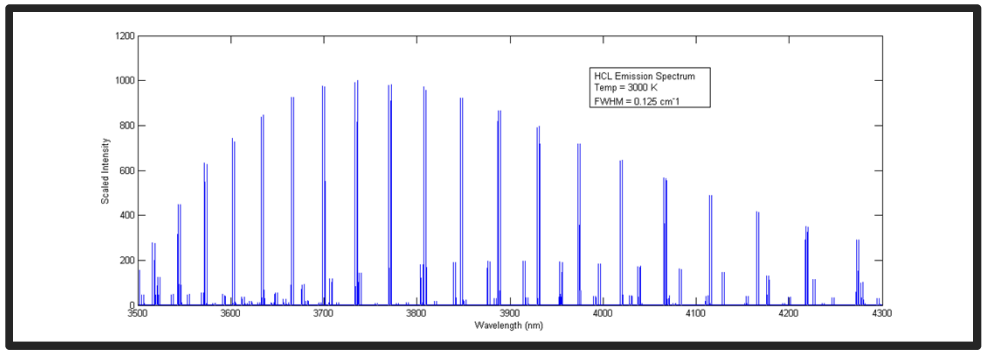

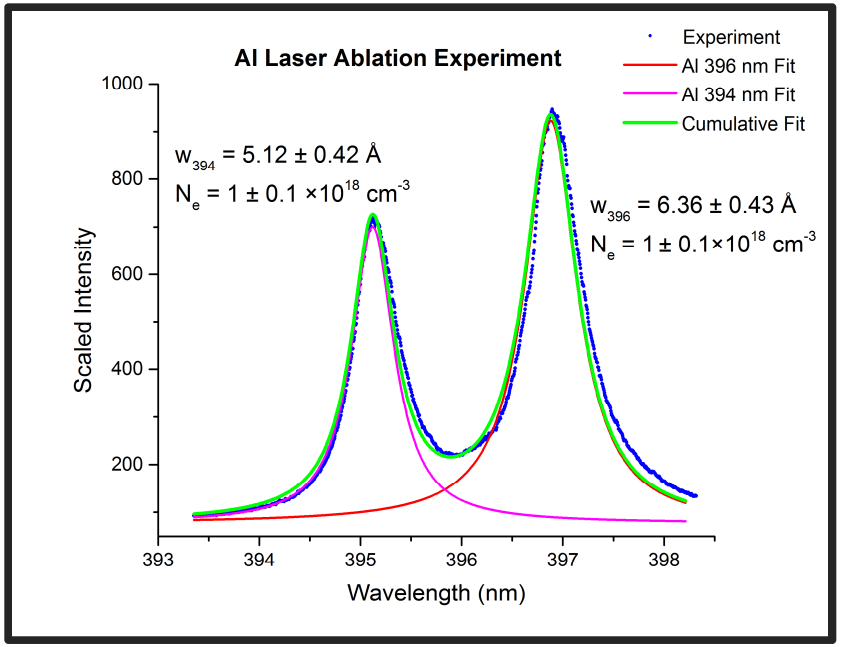

Acknowledgements

- This work is in part supported by the Center for Laser Applications at the University of Tennessee Space Institute and in part by Sandia National Laboratories. Sandia is a multi-program laboratory operated by Sandia Corporation, a Lockheed Martin Company, for the United States Department of Energy National Nuclear Security Administration under contract DEAC0494AL85000.
- Thermal Test Center Staff, Sandia National Laboratories

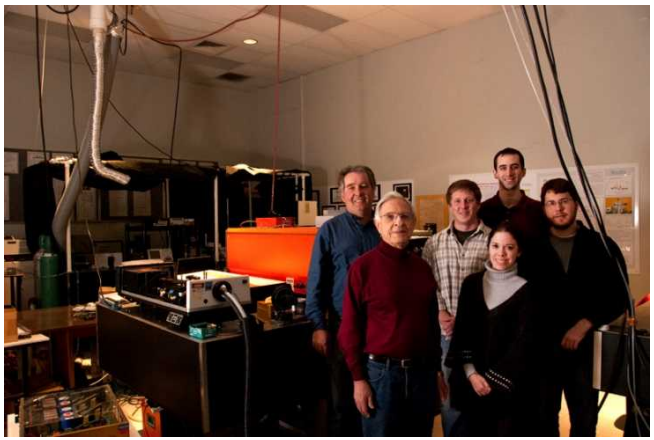

JANNAF

Joint Army-Navy-NASA-Air Force Interagency Propulsion Committee

Sandia National Laboratories

References

1. J.L. Height, B. Donaldson, W. Gill, and C.G. Parigger, “Measurements in solid propellant plumes at ambient conditions,” Proceedings of IMECE2011, Denver, Colorado, USA, 2011, paper IMECE2011-62726.
2. **C.G. Parigger, D.M. Surmick, A.C. Woods, A.B. Donaldson, and J.L. Height. Measurement and analysis of aluminum monoxide emission spectra. 8th US National Meeting of the Combustion Institute. 2013; Park City, UT: paper 305.**
3. **C.G. Parigger, A.C. Woods, D.M. Surmick, A.B. Donaldson, and J.L. Height. Aluminum flame temperature measurements in solid propellant combustion. Appl. Spectroc. 2014; 68:362-366.**
4. **D.M. Surmick, C.G. Parigger, A.C. Woods, A.B. Donaldson, J.L. Height, and W. Gill. Analysis of emission spectra of aluminum monoxide in solid propellant flame. Int. Rev. Atom. Mol. Phys. 2012; 3:137-151.**
5. A. Huag, B.C. Hogan, A.B. Donaldson, C.G. Parigger, D.M. Surmick, “Simulating and Modeling a Solid Rocket Propellant Rocket Plume Using an Aluminum Powder Fed Oxyacetylene Torch,” WSSCI Fall Meeting, Oct. 7-8, 2013, Ft. Collins, CO.
6. **C. F. Bohren and D. R. Huffman, “Absorption and Scattering of Light by Small Particles,” *Wiley, New York, 1983.***
7. **S. M. Stewart, Blackbody Radiation Functions and Polylogarithms, J. Quant. Spectr. and Rad. Trans., 113, 232-238 (2012).**
8. M.R. Weismiller, J.G. Lee, R.A. Yetter, ”Temperature measurements of Al containing nano-thermite reactions using multi-wavelength pyrometry,” Proc. Comb. Inst. 33, 1933-1940 (2011).
9. P. Lynch, H. Krier, and N. Glumac, "Emissivity of Aluminum-Oxide Particle Clouds: Application of Pyromerty of Explosive Fireballs," Journal of Thermophysics and Heat Transfer, 24, 301-308 (2010).
10. S. Goroshin, J. Mamen, A. Higgins, T. Bazyn, N. Glumac, and H. Krier, “Emission Spectroscopy of Flame Fronts in Aluminum Suspensions,” Proceedings of the Combustion Institute, 31, 2011-2019 (2007).
11. **C.G. Parigger. "Measurements of Laser-Induced Plasma and Optical Breakdown Spectra of Aluminum," AIP Conf. Proc. 2006. 874: 101-111.**
12. **C.G. Parigger, J.O. Hornkohl, and L. Nemes. "Measurements of Aluminum and Hydrogen Microplasma," Appl. Opt., 46, 4026-4031 (2007).**
13. I. G. Dors, C. Parigger, and J. W. L. Lewis, “Spectroscopic Temperature Determination of Aluminum Monoxide in Laser Ablation with 266-nm Radiation,” Opt. Lett. **23**, *1778-1780 (1998).*
14. **C. G. Parigger and J. O. Hornkohl, “Computation of AlO $B^2\Sigma^+ \rightarrow X^2\Sigma^+$ Emission Spectra,” Spectrochim. Acta, Part A – Molec. Biomolec. Spectrosc. 81, 404-411 (2011).**